

Research Article

Remote sensing image target detection based on Yolo algorithm

Lianchen Zhao^{1,2}, Yizhun Peng^{1,2}, Di Li^{1,2}, Yuheng Zhang^{1,2}¹College of Electronic Information and Automation, Tianjin University of Science and Technology, China²Advanced Structural Integrity International Joint Research Centre, Tianjin University of Science and Technology, China

ARTICLE INFO

Article History

Received 16 November 2020

Accepted 12 November 2021

Keywords

Deep learning

Target detection

Residual network

Remote sensing image

Feature pyramid

ABSTRACT

There are still some improvements in target detection of high-resolution optical remote sensing images. In this paper, deep learning algorithm is used to detect the target in remote sensing image. Improve and optimize the deep learning target detection algorithm. The concepts of multi-scale feature fusion, feature pyramid and residual network are explained. By improving yolov3 algorithm, the detection effect of aircraft and ship in DOTA data set is significantly improved.

© 2022 The Author. Published by Sugisaka Masanori at ALife Robotics Corporation Ltd.

This is an open access article distributed under the CC BY-NC 4.0 license

[\(http://creativecommons.org/licenses/by-nc/4.0/\)](http://creativecommons.org/licenses/by-nc/4.0/).

1. Introduction

For high-resolution optical remote sensing images, there are still many challenges in target detection. This paper introduces the multi-scale target detection in optical remote sensing images by using Yolov3 [1], and compares the detection results of multi-scale targets on the selected remote sensing data sets by using the improved Yolov3 model.

Target detection is an important direction of computer vision and digital image processing [2]. Target detection has great potential and has good application prospects in robot navigation, real-time vehicle monitoring, industrial defective product detection, aerospace ship detection and so on. Through the algorithm of target detection in deep learning, we can realize the accurate detection of the target, which not only has a great reduction in manpower, but also has a high efficiency improvement, which has important practical significance. Target detection algorithms in deep learning can be divided into two categories: one-stage algorithm and two-stage algorithm [3].

2. One-Stage target detection algorithm

One-Stage, a target detection algorithm based on deep learning, has a faster detection speed when detecting the target [4], because the target detection algorithm discards the process of single region recommendation. This algorithm is first proposed from CVPR 2016, and Yolo (you only look once: unified, real time object detection) is an innovative one stage detection.

The accuracy of the two-stage method is higher than that of the one-stage method, because the two-stage method will form a candidate region and then extract features in the candidate region, but also because of this, the speed of the two-stage method is much lower than that of the one-stage method.

Yolo did not remove the candidate regions [5], but directly divided the input network image into $49 \times 7 \times 7$ grids. Any existing grid predicted two boundary boxes, so as to achieve the prediction of 98 boundary boxes. It can be roughly understood as a rough selection of 98 candidate regions on the input image, which cover the entire region

of the image. Therefore, regression prediction is used to compare the existing 98 candidate boxes to get the final applicable boundary box.

Yolo network draws lessons from the structure of GoogleNet [6] classification network. Compared with GoogleNet classification network, the 1x1 convolution layer and 3x3 convolution layers are used to replace the inception module in Yolo. There are 24 convolution network layers and 2 full connection layers in the whole detection network. Compared with the previous version of Yolo, Yolov3 adjusts the network structure, and uses the Darknet-53 [7] network structure compared with Yolov2. The specific network structure is shown in Figure 1 below:

Type	Filters	Size	Output
Convolutional	32	3 x 3	256 x 256
Convolutional	64	3 x 3 / 2	128 x 128
Convolutional	32	1 x 1	
Convolutional	64	3 x 3	
Residual			128 x 128
Convolutional	128	3 x 3 / 2	64 x 64
Convolutional	64	1 x 1	
Convolutional	128	3 x 3	
Residual			64 x 64
Convolutional	256	3 x 3 / 2	32 x 32
Convolutional	128	1 x 1	
Convolutional	256	3 x 3	
Residual			32 x 32
Convolutional	512	3 x 3 / 2	16 x 16
Convolutional	256	1 x 1	
Convolutional	512	3 x 3	
Residual			16 x 16
Convolutional	1024	3 x 3 / 2	8 x 8
Convolutional	512	1 x 1	
Convolutional	1024	3 x 3	
Residual			8 x 8
Avgpool		Global	
Connected		1000	
Softmax			

Fig. 1. Darknet-53 network structure

In Figure 1, the main structure of the network structure of darknet-53 mainly consists of DBL module, Upsample module, Shortcut module, Res module and Route module. The main components of DBL are convolution network, BN and Leaky relu.

The size of network input image is 416 * 416 * channels. After 5 times of down sampling and 2 times of up sampling stitching through convolution layer, three kinds of feature maps will be output. There are 53 layers of convolutions in the darknet-53 network. Except for the last FC, there are 52 convolutions as the main network model structure. For the low-level convolution layer, the field of vision is relatively small, which is responsible for the detection of small targets. For the deep convolution layer, the field of vision is relatively large, which is responsible for the detection of larger targets.

The activation function adopted by yolov3 is leaky relu. Compared with relu, this activation function sets all negative values to zero. Leaky relu function only gives a non-zero slope to all negative values. The mathematical expression is shown in (1):

$$y_i = \begin{cases} x_i & \text{if } x_i \geq 0 \\ \frac{x_i}{a_i} & \text{if } x_i < 0 \end{cases} \quad (1)$$

The Leaky Relu function image is shown in: Figure 2.

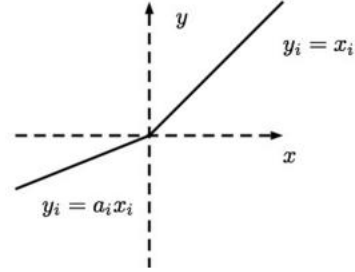


Fig. 2. Leaky Relu function graph

In Yolov3, anchor boxes are needed in bounding box prediction. In Yolov3, K-means clustering algorithm is used to obtain anchors suitable for data sets. The goal of K-means algorithm is to divide n samples into K clusters according to the calculation results [8] so that the similar samples in n samples can be divided into the same cluster. The calculation method used to measure the similarity is to use the size of Euclidean distance (2).

$$d(x, y) = \sqrt{(x_1 - y_1)^2 + (x_2 - y_2)^2 + \dots + (x_n - y_n)^2} = \sqrt{\sum_{i=1}^n (x_i - y_i)^2} \quad (2)$$

The loss function in Yolov3 is shown in formula (3) as follows:

$$\begin{aligned} Loss = & \lambda_{coord} \sum_{i=0}^{S^2} \sum_{j=0}^B I_{ij}^{obj} [(x_i - \hat{x}_i^j)^2 + (y_i - \hat{y}_i^j)^2] + \\ & \lambda_{coord} \sum_{i=0}^{S^2} \sum_{j=0}^B I_{ij}^{obj} [(\sqrt{w_j^j} - \sqrt{\hat{w}_j^j})^2 + (\sqrt{h_j^j} - \sqrt{\hat{h}_j^j})^2] - \\ & \sum_{i=0}^{S^2} \sum_{j=0}^B I_{ij}^{obj} [\hat{C}_i^j \log(C_i^j) + (1 - \hat{C}_i^j) \log(1 - C_i^j)] - \\ & \lambda_{noobj} \sum_{i=0}^{S^2} \sum_{j=0}^B I_{ij}^{noobj} [\hat{C}_i^j \log(C_i^j) + (1 - \hat{C}_i^j) \log(1 - C_i^j)] - \\ & \sum_{i=0}^{S^2} I_{ij}^{obj} \sum_{c \in classes} [\hat{P}_i^j \log(P_i^j) + (1 - \hat{P}_i^j) \log(1 - P_i^j)] \end{aligned} \quad (3)$$

In the above formula, I_{ij}^{obj} is used to determine whether the j anchor box in the i grid is responsible for the current object. If $I_{ij}^{obj} = 1$ is responsible, if $I_{ij}^{obj} = 0$ is not. \hat{C}_i^j parameter is the confidence degree, C_i^j is the real value in the training process. The value of this parameter depends on whether the bounding box of grid cell is responsible for the prediction of an object. If it is responsible for $\hat{C}_i^j = 1$, otherwise, $\hat{C}_i^j = 0$.

Central coordinate error:

$$\sum_{i=0}^{S^2} \sum_{j=0}^B I_{ij}^{obj} [(x_i - \hat{x}_i^j)^2 + (y_i - \hat{y}_i^j)^2] \quad (4)$$

The formula of wide coordinate error in calculation:

$$\sum_{i=0}^{S^2} \sum_{j=0}^B I_{ij}^{obj} [(\sqrt{w_j^i} - \sqrt{\hat{w}_j^i})^2 + (\sqrt{h_j^i} - \sqrt{\hat{h}_j^i})^2] \quad (5)$$

Confidence error:

$$\sum_{i=0}^{S^2} \sum_{j=0}^B I_{ij}^{obj} [\hat{C}_i^j \log(C_i^j) + (1 - \hat{C}_i^j) \log(1 - C_i^j)] - \quad (6)$$

$$\lambda_{noobj} \sum_{i=0}^{S^2} \sum_{j=0}^B I_{ij}^{noobj} [\hat{C}_i^j \log(C_i^j) + (1 - \hat{C}_i^j) \log(1 - C_i^j)]$$

The image pyramid represents a variety of scales of the image. The scale of the image from bottom to top will gradually become smaller, which is similar to the shape of the pyramid, which is very helpful for complex tasks. In yolov3, the understanding of multi-scale detection is that the 1 / 32 feature map (deep layer) has a high sampling multiple, so it has a large receptive field and is suitable for detecting objects with large targets, and 1 / 8 feature map (shallow layer) has a small receptive field, so it is suitable for detecting small targets.

When the network depth becomes deeper and deeper, the training accuracy will become stable, but the training error will become larger and larger. In order to solve this problem, the residual network is proposed. After RESNET is launched, it is no longer necessary to use multiple stacked layers to fit the mapping of expected features, but can directly use a residual mapping.

3. Experimental results and analysis before improving the model

3.1. Experimental process

The target detection process is as follows:

- (1) The experimental data set is preprocessed, and the large-scale remote sensing image is clipped;
- (2) Determine whether the remote sensing image is a single channel image, and select the appropriate defogging processing method;
- (3) Remove the objects that are not interested in the remote sensing data set, and keep the whole data set only contain the two kinds of objects of interest in this paper;
- (4) The processed remote sensing data are input into the network model for training, and the training model is obtained;
- (5) After training, the target is detected and classified.

3.2. Analysis of experimental results

The changes of loss value and val_loss value during training are shown in Figure 3 below:

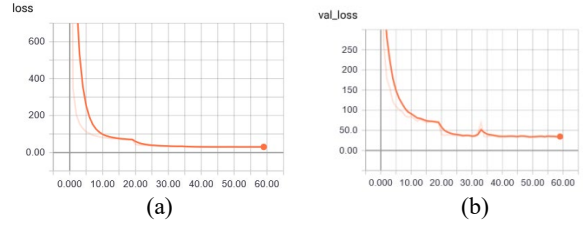


Fig. 3. Changes in loss during training

According to the change of loss value in Figure 3 (a), it can be seen that the loss value changes greatly in the first stage, and gradually decreases and tends to be stable in the second stage. According to the change of loss of verification set in Figure 3 (b), it can be seen that the change of loss value tends to decrease during the training process.

After training, you will get trained_weights_final.h5 file is used to test the test set, set the IOU value to 0.5, and then get the final evaluation result of the training result according to the test results. Since the data set used in this experiment is to integrate part of the data in NWPU VHR-10 remote sensing data set and part of the data in DOTA-v1.5 remote sensing data set, and only contains two types of targets, the detection results are shown in Figure 4, and the test evaluation is shown in Table 1:

Table 1. Evaluation of test set experiment results

Target category	Precision	Recall	AP
plane	0.64	0.93	83.83%
ship	0.71	0.43	40.02%

According to the above Table 1, the AP value of aircraft is 83.83%, the AP value of ship is 40.02%, and the mAP of two types is 61.93%. It is not difficult to see from the results in the table that the detection accuracy of these two types of targets is not high, and the recall rate of ships is much smaller than that of aircraft, which affects the AP value is much smaller than that of aircraft.

4. Experimental results and analysis after improving the model

In this paper, we consider the scale problem to increase the size of the feature map to retain more semantic information on the resolution. By increasing the scale of the input image, more semantic information can be retained. In this paper, the size of the input image is modified to 608 × 608 and 672 × 672.

The prior frame was originally proposed because of Faster R-CNN [9]. According to the size of the ground_truth mark box in the training set, the width and height of the

frequently appeared label box are counted, and these mark boxes are taken as the prior box. In order to make the prior frame suitable for the remote sensing data set used in this experiment, therefore, K-means clustering operations are carried out on the dataset for several times. We use ten times clustering to get ten groups of prior frames, and get the most suitable prior frame by means of average value. As shown in Table 2 below:

Table 2. A priori box improvement

Characteristic	13*13	26*26	52*52
map			
Perception vision	large	medium	small
Initial prior box	(116x90) (156x198) (373x326)	(30x61) (62x45) (59x119)	(10x13) (16x30) (33x23)
Clustering			
mean prior frame	(49x37) (65x67) (125x123)	(31x40) (35x26) (43x30)	(14x27) (21x23) (24x23)

For IOU, IOU is the intersection ratio of detection frame and real frame. In case of non-intersecting border, the gradient will become 0 and cannot be optimized. But for GIOU, this situation can be avoided, so GIOU will be used instead of IOU in this paper. The formula is as follows (7):

$$GIOU = IOU - \frac{|C \setminus (A \cup B)|}{|C|} \quad (7)$$

The loss function of GIOU is shown in formula (8):

$$L_{GIOU} = 1 - GIOU \quad (8)$$

It can be seen from Figure 4 and Figure 5 that on the same data set, the improved model performs better and the loss value is decreasing.

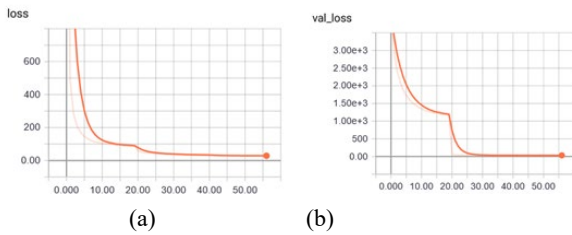


Fig. 4. Change of loss value of input image scale 608x608 after network improvement

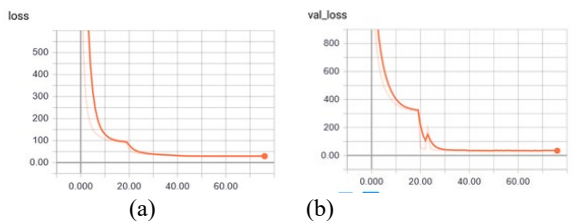


Fig. 5. Change of loss value of input image scale 672x672 after network improvement

As shown in Figure 5, the change trend of the loss value in the network training process is basically consistent. Compared with the input image 608 x 608, the change of the loss value of the verification set with the input image scale of 672 x 672 fluctuates, but the overall trend is that the loss value is gradually reduced.

Combined with the change of prior box, the model is changed to input scale of 672 x 672 and 608 x 608. The number of layers is changed from 52 layers to 56 layers due to the addition of 1 to the layers repeated 8 times in convolution layer. With the increase of input scale and the deepening of network layers, not only more semantic information is retained, but also more semantic information can be extracted in feature extraction. They are shown in Table 3 and Table 4.

Table 3. Comparison of improved network experiment results mAP

network model	Ship AP	Plane AP	mAP
Yolov3	38.60%	86.77%	61.93%
Yolov3_608	42.85%	86.48%	64.69%
Yolov3_672	40.07%	88.94%	64.84%
Yolov3_608_GIOU	40.02%	83.83%	61.93%
Yolov3	38.60%	86.77%	61.93%

Table 4. The improved network Precision and Recall comparison

network model	Ship Precision	Ship Recall	Plane Precision	Plane Recall
Yolov3	0.814	0.411	0.85	0.92
Yolov3_608	0.82	0.448	0.865	0.918
Yolov3_672	0.806	0.433	0.838	0.939
Yolov3_608_GIOU	0.711	0.438	0.648	0.935

The Yolov3_608_GIOU and Yolov3_672_GIOU versions in the above table refer to the replacement of IOU with GIOU based on the Yolov3_608 and Yolov3_672 versions. The yolov3 algorithm, which is not improved, is not effective in small target detection. As can be seen from the above two tables, the recall rate of several improved versions has been improved without much loss of accuracy. Overall, the detection effect of the improved network Yolov3_672_GIOU is the best.

5. Conclusion

This paper first introduces the related concepts of yolov3 algorithm, and then puts forward the concepts of feature pyramid and residual network. Then the yolov3 algorithm is optimized. Firstly, K-means clustering method is used to cluster according to the training set, and then the average value is used as the adjustment of a priori frame. Adjusting the size of the input data picture can extract more semantic

information. Increase the depth of the network and strengthen the training effect. Finally, use GIOU instead of IOU. In the ablation experiment, the detection effect of the improved network Yolov3_672_GIOU is the best, and the mAP is significantly improved.

References

1. Redmon J, Divvala S, Girshick R, et al. You Only Look Once: Unified, Real-Time Object Detection [M]. 2016 IEEE Conference on Computer Vision and Pattern Recognition. 2016:779-88.
2. Felzenszwalb P F, Girshick R B, Mcallester D, et al. Object Detection with Discriminatively Trained Part-Based Models[J]. IEEE Transactions on Software Engineering, 2010, 32(9):1627-1645.
3. Chen L-C, Zhu Y, Papandreou G, et al. Encoder-decoder with atrous separable convolution for semantic image segmentation[C]. Proceedings of the European Conference on Computer Vision (ECCV). 2018: 801 – 818.
4. Liu Chang, Wang Pengjun, Zhang Meiling, et al Research on sparse video detection technology based on IOU analysis [J]. High technology letters, 2019(10).
5. Zhang R, Yao J, Zhang K, et al. S-CNN-BASED SHIP DETECTION FROM HIGH-RESOLUTION REMOTE SENSING IMAGES. [J]. International Archives of the Photogrammetry, Remote Sensing & Spatial Information Sciences, 2016, 41.
6. Walk S, Majer N, Schindler K, et al. New features and insights for pedestrian detection[C]. IEEE Conference on Computer Vision and Pattern Recognition, 2010: 1030-1037.
7. Ok A O, Başeski E. Circular oil tank detection from panchromatic satellite images: a new automated approach[J]. IEEE Geoscience and Remote Sensing Letters, 2015, 12(6): 1347 –1351.
8. Li Weijun. Overview of K-means clustering algorithm [J]. Modern computer (Professional Edition), 2014 (8): 31-32
9. M. Kang, X. Leng, Z. Lin, et al. A modified faster R-CNN based on CFAR algorithm for SAR ship detection[C]. 2017 International Workshop on Remote Sensing with Intelligent Processing (RSIP), Shanghai, China, 2017, 1-4.

Authors Introduction

Mr. Lianchen Zhao



He is currently the master course student in Tianjin University of Science & Technology. His research field is artificial intelligent. His research direction is object detection and deep neural network.

Dr. Yizhun Peng



He is an Associate Professor in Tianjin University of Science & Technology. He received a doctor's degree in control theory and control engineering from the Institute of Automation, Chinese Academy of Sciences, in 2006. His research field is intelligent robot and intelligent control

Mr. Di Li



He is a master graduated in Tianjin University of Science & Technology. His research field is artificial intelligent. His research direction is object detection and data handling

Mr. Yuheng Zhang



He is a third-year master candidate in Tianjin University of Science and Technology, majoring in control engineering. His research field is intelligent robot.